European Journal of Radiology 196 (2026) 112661

Contents lists available at ScienceDirect

European Journal of Radiology

journal homepage: www.elsevier.com/locate/ejrad

Benefits of photon counting CT for the assessment of native heart valves

Charles Mayard [a], Salim Si-Mohamed [a,b], Angèle Houmeau [b], Cyril Prieur [c], Jean-Nicolas Dacher [d,e], Loic Boussel [a,b], Philippe Douek [a,b], Sara Boccalini [a,b,*]

[a] Department of Cardiovascular and Thoracic Radiology, Louis Pradel Hospital, Hospices Civils de Lyon, 59 Boulevard Pinel, Bron 69500, France
[b] University Lyon, INSA-Lyon, University Claude Bernard Lyon 1, UJM-Saint Etienne, CNRS, Inserm, CREATIS UMR 5220, U1206, F-69621, 7 Avenue Jean Capelle O, Villeurbanne 69100, France
[c] Department of Cardiology, Louis Pradel Hospital, Hospices Civils de Lyon, 59 Boulevard Pinel, Bron 69500, France
[d] Department of Cardiovascular and Thoracic Radiology, Charles Nicolle Hospital, CHU de Rouen, Rouen 76000, France
[e] Université de Rouen Normandie, Rouen 76000, France

ARTICLE INFO

Keywords:
Computed tomography angiography
Photon counting CT
Image quality
Heart valves
Calcifications

ABSTRACT

Objectives: Systematic data about whether photon counting detector CT (PCD-CT) could improve the assessment of native heart valves is lacking. Thus, the aim of this study was to assess the performances of PCD-CT for the evaluation of native heart valves as compared to energy integrating detector CT (EID-CT).

Methods: Patients necessitating coronary artery CT were prospectively included (February 2021 to December 2022) to undergo an ECG-gated PCD-CT and EID-CT. A subjective assessment of the sharpness and conspicuity of each of the components of the four valves was performed with a 4-point scale. The number of small structures of the valvular apparati was calculated. The number of calcifications per leaflet and their localization within the thickness of the aortic leaflets were noted. The volume of the calcifications and the full width at mid weight (FWMH) of the aortic valve were calculated.

Results: Thirty-three patients (62 ± 13 years; 88 % men) were included. Conspicuity of aortic, mitral, and pulmonary valvular structures was increased with PCD-CT (all < 0.05) except for the aortic right-non-coronary commissure and the pulmonary right-left commissure ($p = 0.06$ and $p = 0.07$). Sharpness was superior for all the borders and the commissures of the aortic and mitral valve (all $p < 0.05$). More fine structures (nodules, chordae) and calcifications were visible with PCD-CT. The precise localization of the calcifications could be assessed with PCD-CT in most cases (70 %) while the volumes were similar ($p = 0.07$). FWMH was lower with PCD-CT (1.7(IQ = 1.1) vs 2.5 mm (IQ = 1.3); $p < 0.01$).

Conclusions: PCD-CT yielded better subjective and objective image quality of native aortic, mitral and pulmonary valves and allowed for more structures to be detected compared to EID-CT. This might result in earlier, improved diagnosis of valve pathologies.

1. Introduction

Heart valve diseases are a public health problem, particularly in developed countries. In fact, on the one hand they are on the increase, due to the correlation with age, and on the other hand they impair the quality of life, reduce life expectancy in good health and increase the risk of mortality [1,2]. These pathologies are often chronic conditions with a progressive course, the most common being aortic stenosis and mitral insufficiency [2,3]. Infective endocarditis is also of concern, particularly as a result of the increased number of implanted cardiac devices, the improved life-expectancy of patients with congenital heart diseases as well as for its high morbidity and mortality [4–6].

Surgical valve replacement is currently the treatment of choice for severe valvular dysfunction [7]. Nevertheless, percutaneous interventional techniques are also available and are playing an increasingly important role in the management of these patients [8]. In addition,

Abbreviations: CNR, Contrast-to-noise ratio; EID-CT, Energy-integrating detectors CT; CT, Computed tomography; ECG, Electrocardiogram; HU, Hounsfield units; IE, Infective endocarditis; IQ, Interquartile range; LC, Left coronary cusp; NC, Non-coronary cusp; PCD-CT, Photon counting CT; RC, Right coronary cusp; SNR, Signal-to-noise ratio.

* Corresponding author at: Service d'Imagerie Cardio-vasculaire et Thoracique, Hôpital Louis Pradel, Hospices Civils de Lyon, 28 Avenue de Doyen Lépine, Bron 69500, France.
E-mail address: sara.boccalini@chu-lyon.fr (S. Boccalini).

https://doi.org/10.1016/j.ejrad.2026.112661
Received 16 September 2025; Received in revised form 20 December 2025; Accepted 6 January 2026
Available online 7 January 2026

drug therapies are being studied, with the aim of reducing or even revert the calcifying process of the valves [9]. Therefore, accurate and reliable assessment of valves on imaging is essential and a determining factor in the choice of timing and type of treatment. Follow-up will also rely on non-invasive imaging to detect complications. Conventional CT, that is CT systems equipped with energy-integrating detectors (EID-CT), has recently come to play an important role in the diagnosis of valve diseases, in preoperative assessment, in post-intervention monitoring and in the search for extra-cardiac complications [7,10]. Nevertheless, there are still limitations, notably due to the fineness of structures such as the leaflets or cords, which require very high spatial resolution. Also certain artefacts such as blooming artefacts might hamper the interpretation of these examinations if calcifications or metal devices are present. Finally, the temporal resolution of CT systems limits the analysis of moving organs.

CT systems equipped with photon counting detectors (PCD-CT) could overcome some of these limitations having shown to improve spatial resolution and reduce blooming artefacts [11,12], particularly of vascular calcifications and stents [13,14], compared with EID-CT. Additionally, PCD-CT provides better image quality of in vitro mechanical and biological valve prostheses than CT with energy-integrating detectors (EID-CT), providing better sharpness and conspicuity and decreasing metallic and blooming artefacts [15]. However, no data is available for native valves.

Therefore, we sought to assess the additional value of using PCD-CT as compared to EID-CT to analyse anatomical parts as well as calcifications of native heart valves.

2. Material and methods

2.1. Study design

This was a prospective monocentric study carried out in a tertiary University Hospital. Between February 2021 and December 2022, patients with a clinical indication for coronary artery CT were included in the protocol. Each patient underwent CT examinations on both a dual-energy CT with energy-integrating detectors (EID-CT), as part of standard of care, and a photon counting CT prototype, for research, within one month. The study complies with relevant laws and institutional guidelines and have been approved by the appropriate institutional committees and all necessary authorizations have been acquired previous to the beginning of the study. The study was approved by the Ethical Committee of the institution (N ID-RCB: 2019-A02945-52). All patients signed informed consent prior to inclusion. Consecutive patients included in the prospective study during the indicated time period, were later screened for evaluability in the current analysis.

Data about coronary artery image quality, atherosclerosis and stenosis have been previously reported [13,16,17].

2.2. CT systems and CT exams

2.2.1. EID-CT and PCD-CT systems

The EID-CT systems were commercially available first or second generation dual-layer dual-energy CT systems (IQon or CT7500, Philips Healthcare).

The PCD-CT was a clinical prototype with a large field-of-view (FOV of 500 mm in-plane) featuring energy-sensitive photon counting detectors of 2-mm-thick cadmium zinc telluride (CZT), bonded to Philips' proprietary ChromAIX2 application-specific integrated circuit [18]. Pixels dimensions at isocenter are of 270x270 μm^2.

2.2.2. EID-CT and PCD-CT acquisition parameters

An acquisition with retrospective ECG gating was performed with optimized matching parameters on the CT scanners (EID-CT: collimation = 64 × 0.625 or 128 × 0.625 mm, rotation time = 0.27 s, pitch 0.16; PCD-CT: collimation = 64 × 0.275 mm, rotation time = 0.33 s; pitch 0.32). For all systems, the tube voltage was set at 120 kVp with a current fixed at 255 mAs or 330 mAs depending on the size of the patients for PCD-CT while for EID-CT automatic exposure control was used with a DoseRight index of 28 corresponding to a target current at 255 mAs for average adult patient size with water equivalent diameter of 29 cm.

2.2.3. Injection protocol

The injection protocol was the same on the two scanners as previously detailed [13]: 65 or 75 mL of Iomeron 400 mg/mL (Bracco) at 5 mL/sec, depending on the patient's weight, followed by 20 mL at 4 mL/sec of saline. The correct timing of the acquisition after the beginning of the injection was calculated differently on the two CT systems. For EID-CT, bolus tracking was employed. A region of interest (ROI) placed in the descending aorta and a threshold of 110HU. For PCD-CT a bolus test was performed with 20 mL of contrast media at 5 mL/sec followed by 20 mL of saline solution at 4 mL/sec. This difference was due to technical limitations on the PCD-CT prototype and the desire to keep the total volume of contrast media as low as possible.

Unless contraindicated, sublingual spray of nitroglycerin (Natispray; Teofarma SRL) was administered to all patients and an intravenous injection of beta-blockers (esmolol chlorohydrate, Esmocard; Orpha Devel Handels Vertriebs GMBH) was added if the patient's heart rate was judged too high with a target of 65 beats per minute.

2.2.4. Image reconstruction

Images were reconstructed at the phase 78 % of the cardiac cycle for both CT systems. Acquisition and reconstruction parameters for the two systems can be found in Table 1.

2.3. Subjective image quality assessment

For the tricuspid and pulmonary valve, a preliminary analysis about whether the enhancement of the right cavities was sufficient to assess the valve was carried out by a radiologist with 11 years of experience in cardiovascular imaging (xx). In addition, for all valves, the radiologist established whether the image quality, in particular in relation to the presence of motion artefacts, was sufficient to assess at least half of each of the cusps or the scallops of the valve. All valves that were judged not assessable based on these parameters were excluded.

Thereafter, a radiology resident with 6 months experience in cardiovascular imaging (XX) and a radiologist with 11 years' experience in cardiovascular imaging (XX) independently analysed all assessable valves of each patient on the two CT systems. The analysis was carried out with a commercially available solution allowing for multiplanar

Table 1
EID-CT and PCD-CT acquisition and reconstruction parameters.

	EID-CT	PCD-CT
Acquisition parameters		
Collimation [mm]	64x0.625 or 128x0.625	64x0.275
Tube voltage [kV]	120	120
Tube current [mAs]	Reference 255	255 or 330
Dose modulation	DoseRight	None
Rotation time [s]	0.27	0.33
Pitch	0.16	0.32
Reconstruction parameters		
FOV [mm]	220	220
Matrix [pixels]	512x512	1024x1024
Slice thickness [mm]	0.67	0.25
Increment [mm]	0.34	0.25
Voxel size [mm]	0.625(z) x 0.43(x) x 0.43(y)	0.25(z) x 0.21(x) x 0.21(y)
Kernel	XCB and XCD	Detailed 2 and Sharp
Iterative reconstruction	iDose 3	iDose 6

FOV: field of view.

reconstructions (ISP Portal, Philips). At all steps, including the preliminary analysis, the observers were blinded to the type of CT scanner and to any clinical information but were free to change planes, zoom, window level and window width as desired.

Conspicuity and sharpness of the different parts of the valve apparatus were assessed using a 4-point score. For conspicuity the score was: 1 = target structure is not visible or barely visible, image quality is poor; 2 = target structure is located but difficult to interpret; 3 = target structure is well visible but interpretation remains imperfect; 4 = target structure is clearly visible and interpretable. For sharpness the score was: 1 = unacceptable blurring of the borders of the target structure; 2 = suboptimal definition of the borders of the structures; 3 = the borders can be identified with confidence on all their trajectory; 4 = perfect definition of the target structure. Thereafter, the average scores of the two observers were calculated. The inter-observer agreement for the assessment of the aortic and mitral valve per CT system was calculated.

The list of parameters assessed per each valve is reported below.

2.3.1. Aortic valve

- Sharpness and conspicuity of edges and commissures between each cusp (left coronary cusp (LC)-right coronary cusp (RC), RC–non-coronary cusp (NC) and LC–NC), and calcifications regardless of their location.
- Presence of the nodules of Arantius on each leaflet. The nodules of Arantius were defined as a nodular thickening in the middle of the edge of each cusp [19].
- Number of visible calcifications in the valve leaflet (LC, RC, NC), edge or commissure (LC-RC, RC-NC and LC-NC). This evaluation was carried out only by the radiology resident.
- Localization of the calcifications: on the aortic side of the leaflet, across the thickness of the valve (transmural), or of doubtful localization.

2.3.2. Mitral valve

- Sharpness and conspicuity of different parts of the anterior and the posterior leaflet (A1, A2, A3 and P1, P2, P3), nodule of the anterior or posterior valve, attachment of the chordae to the valve, papillary muscles, trabeculations, and calcifications regardless of their location.
- The presence and number of visible chordae originating from the two papillary muscles, separately.
- The presence of calcifications of the following structures: into the different parts of the valves (A1, A2, A3 and P1, P2, P3), and on the annulus.
- Presence and measure of mitral annular disjunction at any location. This was defined as any distance from the top edge of the ventricular wall to the hinge of the leaflet $\geq$ 1 mm [20].

2.3.3. Tricuspid valve

- The number of leaflets
- Sharpness and conspicuity of leaflets (anterior, posterior, and septal), nodules, attachment of the chordae to the valve if visible, and trabeculations.
- The presence and number of visible chordae.

2.3.4. Pulmonary valve

- Sharpness and conspicuity of edges and commissures of the three leaflets (left-anterior, anterior–right and left–right), and calcifications regardless of their location.
- Presence of nodules of Morgagni on each leaflet. The nodules of Morgagni were defined as a nodular thickening in the middle of the edge of each cusp [19].

2.4. Objective image quality assessment

2.4.1. Aortic valve calcifications

A commercially available software was used to identify the aortic annulus (TAVI-planning, ISP Portal, Philips) and to provide a preliminary segmentation of the calcifications of the aortic valve. Thereafter, the segmentation was manually modified to include all calcifications on the leaflets and to exclude all calcifications just above and just below (including those on the aortic annulus) (Fig. 1). Thereafter, the volume of the calcifications and their densities were extracted.

2.4.2. Evaluation of the sharpness of the aortic valve

In order to measure the sharpness of the cusps of the aortic valve, the full width at mid height (FWMH) was calculated: a line was traced perpendicular to the commissure between the left and the right coronary cusps and the profile of attenuation across this line was extracted with an open source software for image analysis (ImageJ, version 1.54 g, U. S. National Institutes of Health, Bethesda, Maryland, USA) (Fig. 2).

2.4.3. Correlation between subjective scores and signal to noise and contrast to noise ratio

Regions of interest were drawn in the aorta just above the aortic valve and in the trachea or proximal bronchi at the same level. The attenuation in Hounsfield Units (HU) and standard deviation values were noted. The signal-to-noise (SNR) and contrast-to-noise (CNR) ratio were calculated with the following formula:

SNR: HU in the aorta/standard deviation in the aorta.

CNR: (HU value in the aorta-HU in the bronchi)/standard deviation in the bronchi.

Thereafter the correlation with subjective scores for conspicuity and sharpness was calculated for both CT systems.

2.5. Statistical analysis

Statistical analysis was performed with SPSS, version 21 (IBM, Armonk, New York, United States).

Continuous variables are presented as average $\pm$ standard deviation or median (interquartile range(IQ)) as appropriate. Normal distribution was verified with Shapiro's test and Q-Q plots. Frequencies were compared with χ^2 test. Wilcoxon signed-ranked test was used to test differences. These comparisons were performed separately without any further correction in this exploratory study where the interest was focused on the pair-wise comparison of the two CT systems. The intra-class correlation coefficient was calculated with a two-way random model. Results are provided with the 95 % confidence interval. Correlation was calculated with the Pearson test. A p value of < 0.05 was considered statistically significant.

3. Results

3.1. Patients' characteristics and radiation dose

In total 33 patients corresponding to 66 scans were analysed (age = 62 $\pm$ 13 years; 29 men, 88 %).

The mean CT dose index delivered with EID-CT was of 33.6 $\pm$ 10.4 mGy (calculated for 31 patients as for 2 patients data was not retrievable from the PACS) vs 30.7 $\pm$ 3.7 mGy for PCD-CT. The mean dose length product was of 681.8 $\pm$ 159.6 mGy*cm for EID-CT, while with PCD-CT it was of 567.8 $\pm$ 67.7 mGy*cm ($p < 0.01$).

3.2. Subjective analysis

Although motion artefacts were found for the mitral valve in 4 cases with PCD-CT and in 3 cases with EID-CT and at for the aortic valve in one case with EID-CT, none was excluded because at least half of each valve cusp or scallop was assessable. Only two commissures of the aortic valve

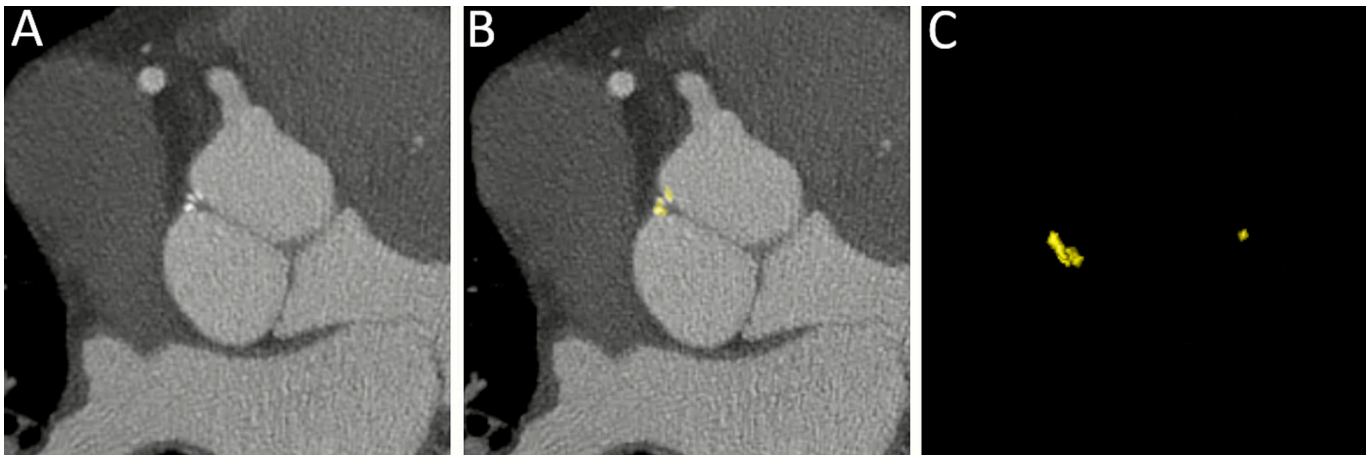

Fig. 1. Measure of calcification volume. A Calcifications on the commissure between the right and non-coronary leaflets. B Results of the segmentation of the calcifications with a dedicated TAVI-planning software, manually modified if inexact. C Tri-dimensional representation of the entire volume of the calcifications as extracted.

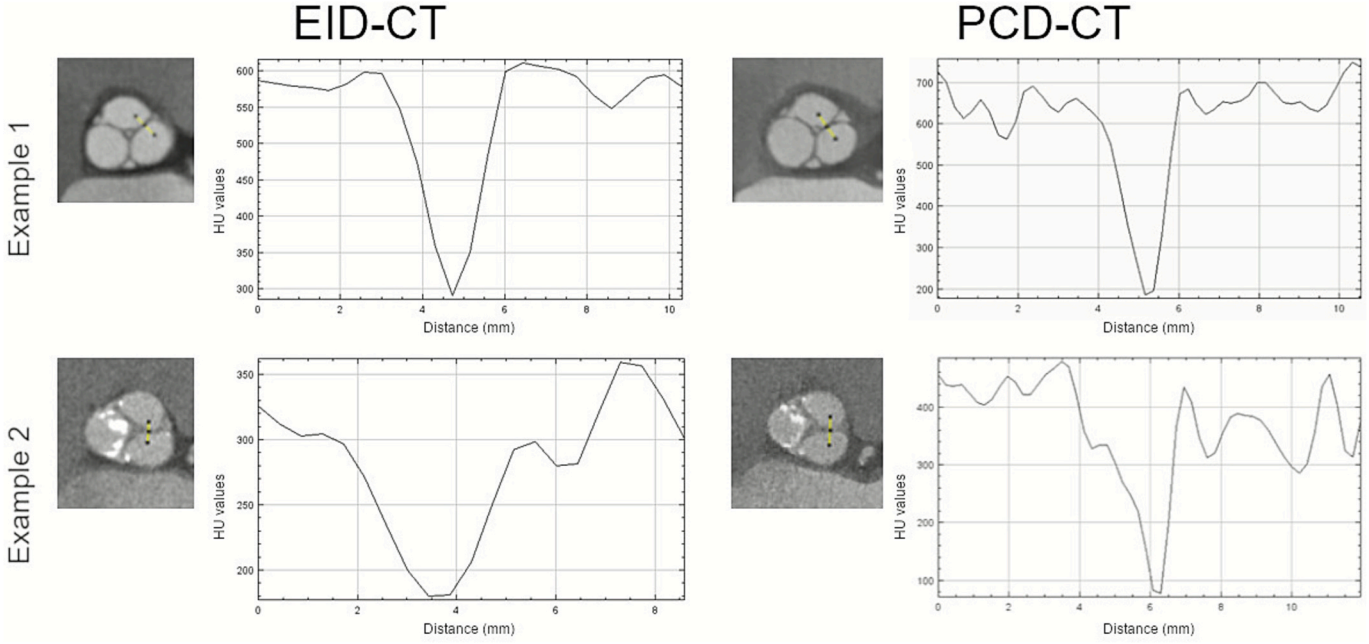

Fig. 2. Evaluation of the objective sharpness of the edge of the cusps of 2 aortic valves. Multiplanar reconstructions of 2 corresponding aortic valves on EID-CT and PCD-CT with graphic representations of the attenuation values along a line drawn cutting the edge between left and right coronary leaflets. Full width at mid height, the parameter we calculated based on these curves, decreases when image sharpness improves, as illustrated in these examples for PCD-CT. Indeed, this parameter is a descriptor of the behaviour of the attenuation curve and low values indicate a narrower curve with more steep slopes. In this study, the differences between the systems are explained mainly by the reduction of partial volume effect with photon counting CT.

had to be excluded from the analysis.

3.2.1. Aortic valve

All aortic valves were tricuspid with the exception of a bicuspid valve, type 0 AP.

The scores of both conspicuity and sharpness of all structures and of calcifications were higher with PCD-CT (all $p < 0.05$) with the exception of the conspicuity of the commissure RC-NC that was well visible on both CT systems (2 (IQ = 1) vs 3 (IQ = 1); $p = 0.6$) (Fig. 3). An example of aortic valve with moderate thickening of the leaflets with the two systems is shown in Fig. 4 and an example of irregular profile of one of the cusps in Fig. 5.

With PCD-CT a total of 31 nodules of Arantius were detected vs 4 with EID-CT. No difference was noted between the observers for either EID-CT ($p = 0.613$) or PCD-CT ($p = 1$).

In addition, 45 calcifications were detected with PCD-CT in 12 patients, whereas 34 calcifications were found with EID-CT ($p = 0.024$). The number and location of the calcifications are reported in Table 2. With EID-CT the localization of the calcifications in the thickness of the leaflets was doubtful in more cases as compared to PCD-CT ($p = 0.02$) (Fig. 6). In addition, the number of calcifications that were limited to the aortic side of the leaflet was higher with PCD-CT ($p = 0.011$). Some examples of aortic valve calcifications as visualized with both CT systems are shown in Fig. 7.

The inter-observer agreement was substantial to almost perfect with EID-CT and almost perfect with PCD-CT (Table 3).

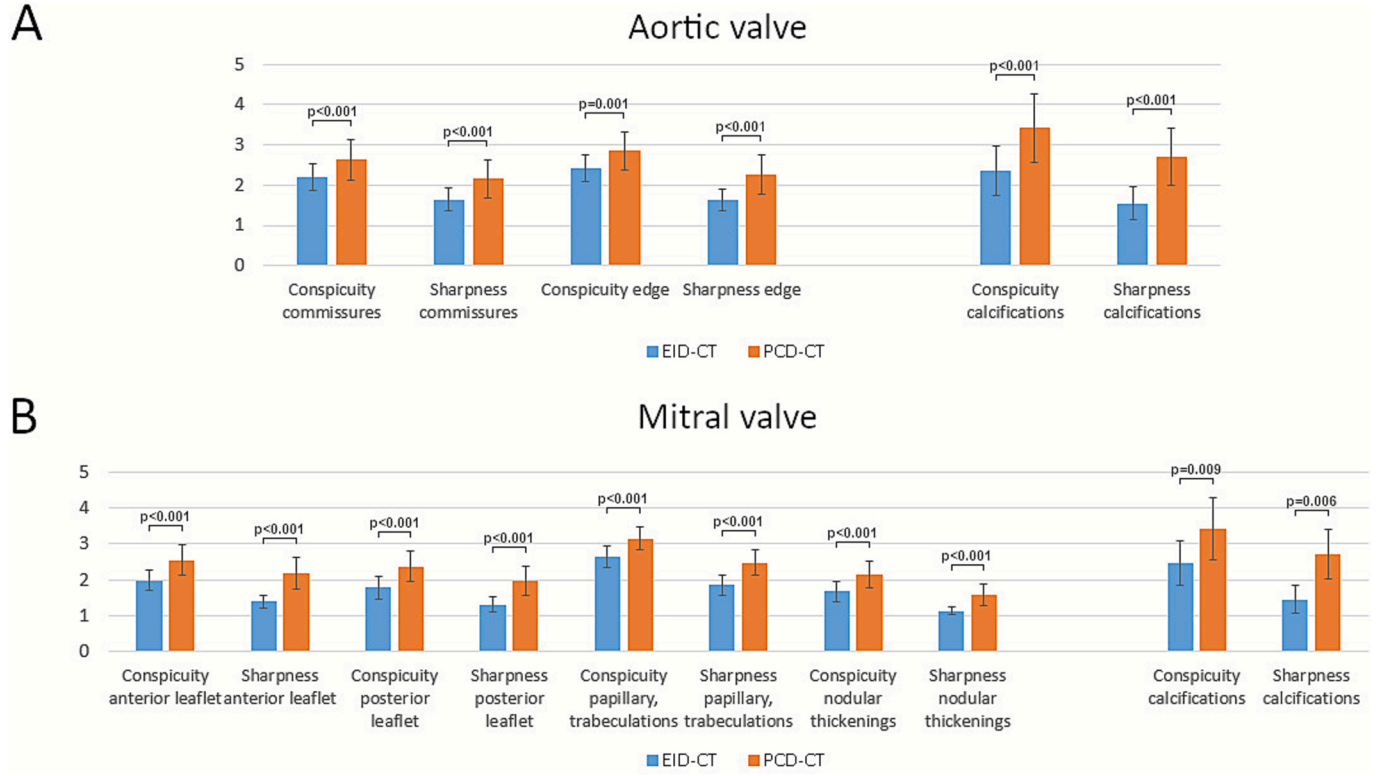

Fig. 3. Bar graphs of subjective scores regarding conspicuity and sharpness of different parts of the aortic (A) and mitral (B) valves and calcifications on the two valves, on EID-CT and PCD-CT.

3.2.2. Mitral valve

Both conspicuity and sharpness of the three parts of each leaflet, the nodules, the thickening at the level of the attachments of the chordae, the papillary muscles, the trabeculations scored significantly higher with PCD-CT (all $p < 0.01$) (Fig. 3). Examples of image quality of different structures of the mitral valve apparatus with EID-CT and PCD-CT are reported in Fig. 5.

A mitral annular disjunction was found in 9 and 13 cases with EID-CT and PCD-CT respectively. The distance was not significantly different between the two systems (2 (IQ = 1) vs 2 (IQ = 0) for EID-CT and PCD-CT, respectively; $p = 0.3$).

More calcifications were detected with PCD-CT (39 vs 30 with EID-CT), particularly on the leaflets (15 vs 9) (Table 2).

The inter-observer agreement was substantial with EID-CT and substantial to almost perfect with PCD-CT (Table 3).

3.2.3. Pulmonary valve

For 18 patients the opacification of the right ventricle and of the pulmonary artery was judged sufficient to analyse the valve for both CT systems.

Significant differences between EID-CT and PCD-CT were found for the conspicuity of all the structures (all $p < 0.05$) with the exception of the commissure between the right and the left cusps ($p = 0.07$). The sharpness was judged superior for PCD-CT only for the edge between the left and the anterior cusps and the edge between the right and the left cusps ($p < 0.05$).

Three nodules of Morgagni were visible with EID-CT and 8 with PCD-CT. No calcifications were visible on the pulmonary valves with either method.

3.2.4. Tricuspid valve

The tricuspid valve was judged assessable in only two cases, both with PCD-CT. Therefore, no further analysis was carried out.

3.3. Objective analysis

3.3.1. Aortic valve calcifications

The total volume of calcifications was similar with the two CT systems ($p = 0.12$). To account for the higher number of calcifications with PCD-CT, the average volume of the calcifications was calculated and compared between EID-CT and PCD-CT yielding a non-significant difference (20 mm^3 (IQ = 17) vs 8.6 mm^3 (IQ = 10); $p = 0.07$).

3.3.2. Aortic valve sharpness

Calculations of the FWMH of the aortic valve were carried out for 32 patients since for one patient the opacification of the aorta on PCD-CT was judged insufficient to extract reliable information. In only one case the commissure that was analysed was the RC-NC due to the fact that the LC-RC was pathological.

The FWMH was smaller for PCD-CT as compared to PCD-CT (1.7 mm (IQ = 1.1) vs 2.5 mm (IQ = 1.3); $p < 0.01$) demonstrating the sharper aspect of the aortic valve on PCD-CT. Some examples are shown in Fig. 2.

3.3.3. Correlation between subjective and objective image quality parameters

For both EDI-CT and PCD-CT, the correlation between the SNR and conspicuity and sharpness scores was moderate for the aortic valve ($\rho = 0.418$, $p < 0.001$ and $\rho = 0.417$, $p < 0.001$; $\rho = 0.437$, $p < 0.001$ and $\rho = 0.414$, $p < 0.001$) and weak for the mitral valve ($\rho = 0.333$, $p < 0.001$ and $\rho = 0.262$, $p < 0.001$; $\rho = 0.368$, $p < 0.001$ and $\rho = 0.246$, $p < 0.001$).

Similarly, the correlation between the CNR and conspicuity and sharpness scores was weak to moderate for the aortic valve ($\rho = 0.371$, $p < 0.001$ and $\rho = 0.292$, $p < 0.001$; $\rho = 0.412$, $p < 0.001$ and $\rho = 0.326$, $p < 0.001$) and very weak to weak for the mitral valve ($\rho = 0.192$, $p < 0.001$ and $\rho = 0.241$, $p < 0.001$; $\rho = 0.239$, $p < 0.001$ and $\rho = 0.250$, $p < 0.001$) for both CT systems.

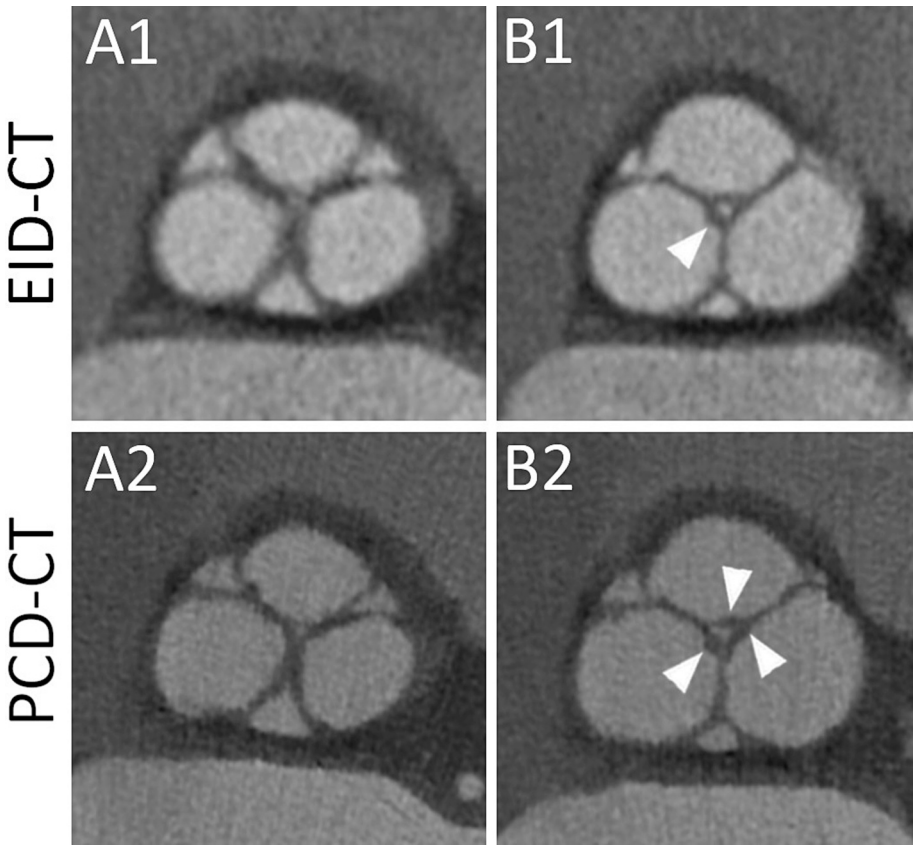

Fig. 4. Corresponding images of the aortic valve of the same patient obtained with EID-CT and PCD-CT. Multiplanar reconstructions showing the aortic valve at two different levels (A1 and A2 show the first level; B1 and B2 show the second level) with EID-CT and PCD-CT (fisrt and second line, respectively). The commissures and the edges of the cusps are thickened and, thus, clearly visible with both modalities. However, they appear sharper with PCD-CT in all their parts, including the focal heterogeneities. In addition, while with EID-CT only one nodule of Arantius is visible (arrowhead, B1), with PCD-CT all three of them are visible (arrowheads, B2).

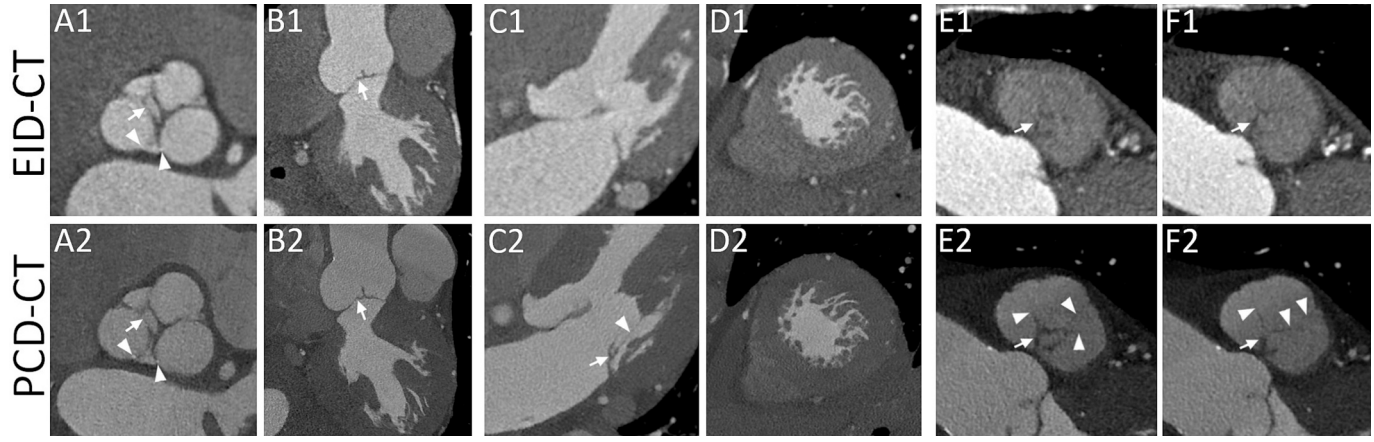

Fig. 5. Examples of aortic (A and B), mitral (C and D) and pulmonary (E and F) valves of the same patient with EID-CT (first line) and PCD-CT (second line). A and B: multiplanar reconstructions perpendicular (As) and parallel (Bs) to the aortic root show an irregular profile of the non-coronary cusp (arrows). The cusps, the commissures and this irregular zone of the aortic valve are sharper with PCD-CT. In addition, some tiny calcifications (A1 and A2, arrowheads) are well visible with PCD-CT but hardly so with EID-CT. C and D: four-chambers (Cs) and short axis (Ds) plane reconstructions of the mitral valve and of the left ventricle trabeculations allow to appreciate the better conspicuity and sharpness of these structures with PCD-CT. In particular, with PCD-CT one entire chordae (C2, arrowheads) and its insertion on the posterior leaflet of the mitral valve were clearly visible, whereas with EID-CT only the position of the insertion point can be guessed when knowing it is there. E and F: multiplanar reconstructions passing on planes perpendicular to the pulmonary trunk at different levels of the pulmonary valve. With both EID-CT and PCD-CT the edges of the cusps appear thickened but with PCD-CT they are more clearly visible and sharper. In addition, only with PCD-CT the commissures are visible (arrowheads).

4. Discussion

In our study, the sharpness and conspicuity of most of the different structures of the cardiac valvular apparati were both improved with PCD-CT compared to EID-CT. Small structures, such as the Arantius nodules, were more often detected with PCD-CT than with EID-CT. With

Table 2
Quantification of structures with the two CT systems (sum of findings of the two observers).

	EID-CT	PCD-CT
Aortic valve		
Nodules of Arantius	4	31
Calcifications		
Total	34	45
Cusps	24	31
Commissures	10	14
Mitral valve		
Calcifications		
Total	30	39
Annulus	21	24
Leaflets	9	15
Chordae		
From anterior papillary muscle	109	164
From posterior papillary muscle	40	88

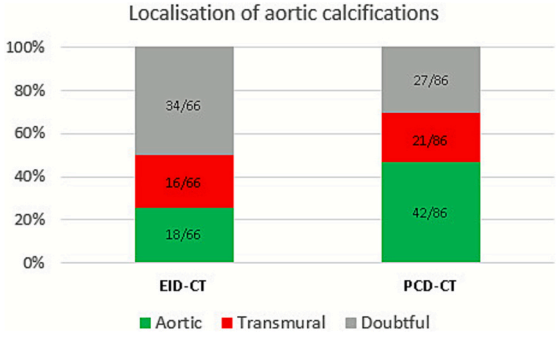

Fig. 6. Graphs showing the results of the assessment of the localisation of aortic valve calcifications. The values overwritten in the graphs indicate the ratio of the number of calcifications per localization over the total number of calcifications detectable with that CT system for both observers.

PCD-CT, more aortic and mitral calcifications were detected, and their precise location within the thickness of the aortic valve leaflets was established with less doubts.

Current guidelines highlight the important role of cardiac CT for pre-interventional and pre-surgical planning [7]. It has been shown recently that PCD-CT systems provide better subjective image quality and more interpretable CT examinations for transcatheter aortic valve implantation planning as compared to EID-CT [21]. Although CT allows to derive most necessary measurements for many interventions, many repair and mini-invasive procedures could probably be better planned and realized if more information were available about the anatomy of the valve and subvalvular apparatus. One example is represented by the chordae of the mitral valve at their junction to the scallops [22,23]. The importance of these structures is highlighted by their inclusion in several scores for echocardiographic assessment of the mitral valve, including the Wilkins's one [24,25]. Nevertheless, the limits of echocardiography for this type of evaluation were largely described and acknowledged [25,26]. We demonstrated that with PCD-CT more of these small structures are visible. Our results are consistent with recent studies showing improved visibility of prosthetic valve structures [15], and, more generally, better visualization of thin structures [12]. Due to the novelty of our investigations, a comparison of the current findings with data from the literature is not possible. In the light of our results, using PCD-CT for the evaluation of native heart valves could improve the initial diagnostic work-up as well as the pre-operative or pre-interventional planning in case prosthetic replacement or valve repair is deemed necessary.

Similarly, new medical or interventional therapies for aortic stenosis, directly promoting resorption or physical destruction and elimination of the calcifications [27,28], might benefit from the improved detection of

Table 3
Inter-reader agreement for subjective analysis of the aortic and mitral valves.

	EID-CT		PCD-CT	
	ICC	CI 95 %	ICC	CI 95 %
Aortic valve				
Conspicuity	0.809	0.688–0.883	0.885	0.812–0.930
Sharpness	0.739	0.574–0.840	0.894	0.827–0.935
Mitral valve				
Conspicuity	0.794	0.709–0.854	0.840	0.774–0.887
Sharpness	0.739	0.574–0.840	0.791	0.703–0.852

CI: confidence interval. ICC: intraclass correlation coefficient.

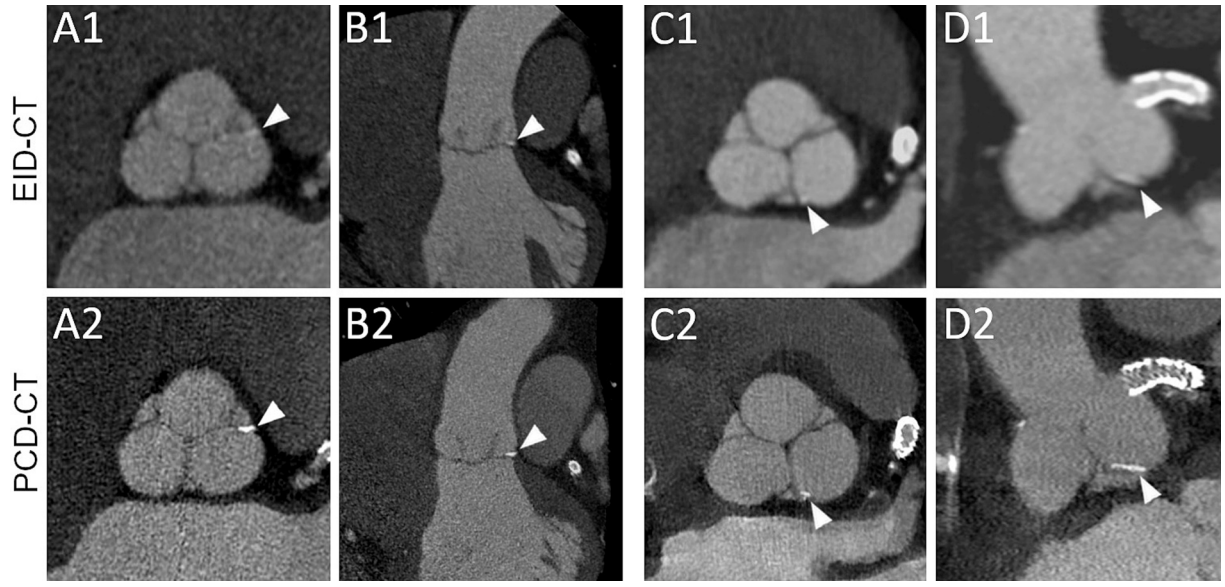

Fig. 7. Corresponding images of aortic valvular calcifications of two patients obtained with EID-CT and PCD-CT. Two multiplanar reconstructions of a first aortic valve showing a small linear calcification on the commissure between the left and right cusps (arrowheads A1, A2, B1, B2). Two multiplanar reconstructions of a second aortic valve showing a linear calcification on the commissure between the left and non-coronary cusps (arrowheads C1, C2, D1, D2), almost invisible on EID-CT and easy to detect on PCD-CT. Both patients had stents in the left coronary artery.

valvular calcifications with PCD-CT. The mechanism of calcifying pathology in the aortic valve is still under investigation and research results suggest that it is a complex, progressive process that affects the aortic side of the leaflets at first, then progressively transfixes the entire thickness of the leaflet [29]. Drug and interventional treatments aiming to resorb these calcifications in situ are being studied. Precise assessment of the presence, density, structure and changes over time of all these parameters will be fundamental. CT is considered the only imaging modality that allows for detailed non-invasive analysis and quantification of calcifications [30]. Nevertheless, it suffers from important limitations including the limited spatial resolution, the poor contrast resolution, making the distinction of feebly dense calcifications from contrast media difficult if not impossible, and blooming artefacts, that by definition, do not permit to estimate correctly the volume, density and structure of calcifications [31,32]. In the current study, we were able to detect a greater number of mitral and aortic valve calcifications with PCD-CT, in accordance with previous studies conducted on in-vitro calcifications [33]. The calcifications visible on PCD-CT and not visible on EID-CT appear to be the smaller, less dense calcifications as shown in examples from the current study and from previous phantom assessment [33]. Moreover, in the case of transfixing calcifications, their resorption would leave an orifice within the leaflet possibly causing valvular insufficiency [9,34]. Therefore, assessing the localization of these calcifications with good confidence would be fundamental.

Interestingly, in our study we did not find any statistically significant difference in the volume of calcifications as calculated with the two CT systems. This result could be explained by several factors. Firstly, a relatively small number of patients with aortic valve calcifications reduced the statistical power of this comparison. Secondly, for the above-mentioned reasons, some calcifications and some parts of the calcifications, the less dense ones, are not detected with the EID-CT whereas they are with PCD-CT, thus reducing the total volume measured by the EID-CT.

The diagnosis of infective endocarditis (IE), is often complex and relies on several criteria, such as the detection of valvular and paravalvular lesions with non-invasive imaging modality. Based on the latest guidelines, these imaging modalities include echocardiography, transthoracic and transesophageal, cardiac CT and PET-CT [4]. These techniques present different strengths and weaknesses. For instance, compared to echocardiography, the performances of CT are better for the detection of paravalvular lesions and worse for vegetations [35]. Although we did not analyse patients with IE in this study, we have shown the possibility of detecting very small structures on the mobile leaflets thanks to PCD-CT, with a greater number of Arantius and Morgagni nodules detected as compared to EID-CT. Sharpness and conspicuity of the attachment of the chordae on the mitral valve were also improved. This leads us to believe that the improved spatial resolution of PCD-CT compared with EID-CT could be of interest in the identification of vegetations attached to the valves.

To take advantage of the technical features of PCD-CT, reconstructions have to be performed with high matrix, small slice thickness and adapted kernels. The importance of choosing the correct parameters has already been highlighted by several articles using different photon counting CT systems [36–38]. As a consequence, also a specific but more irradiating acquisition protocol allowing for this type of reconstructions has to be used with some PCD-CT systems [39]. In the present study, we used previously established dedicated acquisition and reconstruction parameters that were chosen on the one hand to be comparable between the two CT systems and, on the other, to exploit the higher spatial resolution and artefact reduction offered by the PCD-CT [37]. It would be interesting to compare different parameters and different kernels in further research.

The most important limitation of our study is that we included patients undergoing a cardiac CT for a clinical indication of coronary artery disease assessment. Therefore, we studied a limited number of abnormal heart valves, mainly calcifications, and almost no severe heart valve diseases. In addition, the search for coronary pathology requires systemic arterial opacification, and opacification of the right cavities was often insufficient for right valve assessment. Therefore, no data about the tricuspid could be provided and the data on the pulmonary valve should be regarded with caution due to the small cohort analysed. In addition, the opacification of the 4 chambers of the heart was not exactly the same for the two exams. The smaller detector coverage on the PCD-CT as compared to the EID-CT should be considered a technical limitation. Nevertheless, we did not exclude any patients from the analysis for extensive motion artefacts and our results still show better image quality for PCD-CT. Due to the matching of acquisition parameters with the two CT systems, retrospectively ECG gated acquisitions were performed for all patients resulting in relatively high radiation doses for EID-CT, albeit in line with data from the literature [40,41]. Finally, we performed our analysis only in one phase of the cardiac cycle. This means that some details of the mitral valve apparatus were possibly more difficult to assess due to the open position and, surely, that we could not evaluate the benefits of PCD-CT for the depiction of the valve motility and dynamic changes.

In conclusion, photon counting CT provided better image quality of native aortic, mitral and pulmonary valves and the mitral subvalvular apparatus than EID-CT. Its routine use could improve the analysis of heart valve diseases in terms of diagnosis, pre-therapy assessment and follow-up. In addition, PCD-CT allowed for improved detection of calcifications and easier assessment of their location within the leaflets of the aortic valve, which will likely improve diagnostic accuracy and reproducibility during follow-up ultimately helping, for instance, in the investigation of new therapies.

Disclosures

S S-M, PD, SB reported receiving personal and institutional speaker fees from Philips Healthcare, not related to the content of this manuscript.

CRediT authorship contribution statement

Charles Mayard: Writing – review & editing, Writing – original draft, Visualization, Methodology, Formal analysis, Data curation. **Salim Si-Mohamed:** Investigation. **Angèle Houmeau:** Investigation, Data curation. **Cyril Prieur:** Investigation. **Jean-Nicolas Dacher:** Writing – review & editing. **Loic Boussel:** Writing – review & editing. **Philippe Douek:** Project administration, Funding acquisition. **Sara Boccalini:** Writing – review & editing, Visualization, Validation, Supervision, Methodology, Investigation, Formal analysis, Data curation, Conceptualization.

Funding

European Union Horizon 2020 research and innovation program; grant No. 668142.

Declaration of competing interest

The authors declare the following financial interests/personal relationships which may be considered as potential competing interests: SSM, PD and SB received speaker fees from Philips Healthcare in the past. The other authors reported no conflict of interest.

References

[1] V.T. Nkomo, J.M. Gardin, T.N. Skelton, J.S. Gottdiener, C.G. Scott, M. Enriquez-Sarano, Burden of valvular heart diseases: a population-based study, Lancet 368 (2006) 1005–1011, https://doi.org/10.1016/S0140-6736(06)69208-8.

[2] S. Yadgir, C.O. Johnson, V. Aboyans, O.M. Adebayo, R.A. Adedoyin, M. Afarideh, et al., Global, regional, and national burden of calcific aortic valve and degenerative

mitral valve diseases, 1990-2017, Circulation 141 (2020) 1670–1680, https://doi.org/10.1161/CIRCULATIONAHA.119.043391.
[3] T.J. Cahill, A. Prothero, J. Wilson, A. Kennedy, J. Brubert, M. Masters, et al., Community prevalence, mechanisms and outcome of mitral or tricuspid regurgitation, Heart 107 (2021) 1003–1009, https://doi.org/10.1136/heartjnl-2020-318482.
[4] V. Delgado, N. Ajmone Marsan, S. de Waha, N. Bonaros, M. Brida, H. Burri, et al., 2023 ESC guidelines for the management of endocarditis, Eur. Heart J. 44 (2023) 3948–4042, https://doi.org/10.1093/eurheartj/ehad193.
[5] S. Momtazmanesh, S. Saeedi Moghaddam, E. Malakan Rad, S. Azadnajafabad, N. Ebrahimi, E. Mohammadi, et al., Global, regional, and national burden and quality of care index of endocarditis: the global burden of disease study 1990–2019, Eur. J. Prev. Cardiol. 29 (2022) 1287–1297, https://doi.org/10.1093/eurjpc/zwab211.
[6] G. Habib, P.A. Erba, B. Iung, E. Donal, B. Cosyns, C. Laroche, et al., Clinical presentation, aetiology and outcome of infective endocarditis. results of the ESC-EORP EURO-ENDO (European infective endocarditis) registry: a prospective cohort study, Eur. Heart J. 40 (2019) 3222–3232B, https://doi.org/10.1093/eurheartj/ehz620.
[7] A. Vahanian, F. Beyersdorf, F. Praz, M. Milojevic, S. Baldus, J. Bauersachs, et al., 2021 ESC/EACTS guidelines for the management of valvular heart disease: developed by the Task Force for the management of valvular heart disease of the European Society of Cardiology (ESC) and the European Association for Cardio-Thoracic Surgery (EACTS), Rev. Esp Cardiol. (engl Ed) 75 (2022) 524, https://doi.org/10.1016/j.rec.2022.05.006.
[8] S.W. Grant, G.L. Hickey, P. Ludman, N. Moat, D. Cunningham, M. de Belder, et al., Activity and outcomes for aortic valve implantations performed in England and Wales since the introduction of transcatheter aortic valve implantation, Eur. J. Cardio Thoracic Surg. 49 (2016) 1164–1173, https://doi.org/10.1093/ejcts/ezv270.
[9] Feldmann A, Nitschke Y, Linß F, Mulac D, Stücker S, Bertrand J, et al. Improved Reversion of Calcifications in Porcine Aortic Heart Valves Using Elastin-Targeted Nanoparticles 2023.
[10] Baumgartner H, Falk V, Bax JJ, De Bonis M, Hamm C, Holm PJ, et al. 2017 ESC/EACTS Guidelines for the management of valvular heart disease. vol. 38. 2017. 10.1093/eurheartj/ehx391.
[11] P.C. Douek, S. Boccalini, E.H.G. Oei, D.P. Cormode, A. Pourmorteza, L. Boussel, et al., Clinical applications of photon-counting CT: a review of pioneer studies and a glimpse into the future, Radiology 309 (2023) e222432, https://doi.org/10.1148/radiol.222432.
[12] S.A. Si-Mohamed, S. Boccalini, M. Villien, Y. Yagil, K. Erhard, L. Boussel, et al., First experience with a whole-body spectral photon-counting CT clinical prototype, Invest. Radiol. 58 (2023) 459–471, https://doi.org/10.1097/RLI.0000000000000965.
[13] S. Boccalini, S.A. Si-Mohamed, H. Lacombe, A. Diaw, M. Varasteh, P.A. Rodesch, et al., First in-human results of computed tomography angiography for coronary stent assessment with a spectral photon counting computed tomography, Invest. Radiol. 57 (2022) 212–221, https://doi.org/10.1097/RLI.0000000000000835.
[14] G. Fahrni, S. Boccalini, A. Mahmoudi, H. Lacombe, A. Houmeau, M. Elbaz, et al., Quantification of coronary artery stenosis in very-high-risk patients using ultra-high resolution spectral photon-counting CT, Invest. Radiol. 00 (2024), https://doi.org/10.1097/RLI.0000000000001109.
[15] S. Boccalini, C. Mayard, H. Lacombe, M. Villien, S. Si-Mohamed, F. Delahaye, et al., Ultra-high-resolution and K-edge imaging of prosthetic heart valves with spectral photon-counting CT, Invest. Radiol. 59 (2024) 589–598, https://doi.org/10.1097/RLI.0000000000001068.
[16] I. Zadrazil, C. Corzo, V. Voulgaropoulos, C.N. Markides, X.Y. Xu, A combined experimental and computational study of the flow characteristics in a Type B aortic dissection: effect of primary and secondary tear size, Chem. Eng. Res. Des. 160 (2020) 240–253, https://doi.org/10.1016/j.cherd.2020.05.025.
[17] S.A. Si-Mohamed, S. Boccalini, H. Lacombe, A. Diaw, M. Varasteh, P.A. Rodesch, et al., Coronary CT angiography with photon-counting CT: first-in-human results, Radiology 303 (2022) 303–313, https://doi.org/10.1148/RADIOL.211780.
[18] R. Steadman, C. Herrmann, A. Livne, Nuclear instruments and methods in physics research a ChromAIX2 : a large area , high count-rate energy-resolving photon counting ASIC for a spectral CT prototy, Nucl. Inst. Methods Phys. Res. A 862 (2017) 18–24, https://doi.org/10.1016/j.nima.2017.05.010.
[19] H. Gray, Gray's Anatomy: the Anatomical Basis of Clinical Practice, Elsevier, 2016.
[20] D. Zugwitz, K. Fung, N. Aung, E. Rauseo, C. McCracken, J. Cooper, et al., Mitral annular disjunction assessed using CMR imaging: insights from the UK biobank population study, JACC Cardiovasc. Imaging 15 (2022) 1856–1866, https://doi.org/10.1016/j.jcmg.2022.07.015.
[21] T. Dirrichs, J. Schröder, M. Frick, M. Huppertz, R. Iwa, T. Allmendinger, et al., Photon-counting versus dual-source CT for transcatheter aortic valve implantation planning, Acad. Radiol. (2024) 1–10, https://doi.org/10.1016/j.acra.2024.06.014.
[22] A. Vahanian, M. Urena, H. Ince, G. Nickenig, Mitral valve: repair/clips/cinching/chordae, EuroIntervention 13 (2017) AA22–AA30, https://doi.org/10.4244/EIJ-D-17-00505.
[23] J.F. Obadia, C. Casali, J.F. Chassignolle, M. Janier, Mitral subvalvular apparatus, Circulation 96 (1997) 3124–3128, https://doi.org/10.1161/01.cir.96.9.3124.
[24] G.T. Wilkins, A.E. Weyman, V.M. Abascal, P.C. Block, I.F. Palacios, P. House, Percutaneous balloon dilatation of the mitral valve: an analysis of echocardiographic variables related to outcome and the mechanism of dilatation requests for reprints to Dr Arthur E Weyman, Cardiac Noninvasive, Br. Hear J. 60 (1988) 299–308.
[25] O.I.I. Soliman, A.M. Anwar, A.K. Metawei, J.S. McGhie, M.L. Geleijnse, F.J. Ten Cate, New scores for the assessment of mitral stenosis using real-time three-dimensional echocardiography, Curr. Cardiovasc. Imaging Rep. 4 (2011) 370–377, https://doi.org/10.1007/s12410-011-9099-z.
[26] S. Robinson, L. Ring, D.X. Augustine, S. Rekhraj, D. Oxborough, A. Harkness, et al., The assessment of mitral valve disease: a guideline from the British Society of Echocardiography, Echo Res. Pract. 8 (2021) G87–G, https://doi.org/10.1530/ERP-20-0034.
[27] Donato M, Ferri N, Lupo MG, Faggin E, Rattazzi M. Current Evidence and Future Perspectives on Pharmacological Treatment of Calcific Aortic Valve Stenosis 2020.
[28] E. Messas, A. Ijsselmuiden, G. Goudot, S. Vlieger, S. Zarka, E. Puymirat, et al., Feasibility and performance of noninvasive ultrasound therapy in patients with severe symptomatic aortic valve stenosis: a first-in-human study, Circulation 143 (2021) 968–970, https://doi.org/10.1161/CIRCULATIONAHA.120.050672.
[29] A. Rutkovskiy, A. Malashicheva, G. Sullivan, M. Bogdanova, A. Kostareva, K. O. Stensløkken, et al., Valve interstitial cells: the key to understanding the pathophysiology of heart valve calcification, J. Am. Heart Assoc. 6 (2017) 1–23, https://doi.org/10.1161/JAHA.117.006339.
[30] Pawade T, Sheth T, Guzzetti E, Dweck MR. Why and How to Measure Aortic Valve Calci fi cation in Patients With Aortic Stenosis Why and How to Measure Aortic Valve Calci fi cation in Patients With Aortic Stenosis 2019;12. 10.1016/j.jcmg.2019.01.045.
[31] K. Taguchi, A. Khaled, Artifacts in cardiac computed tomographic images, J. Am. Coll. Radiol. 6 (2009) 590–593, https://doi.org/10.1016/j.jacr.2009.05.001.
[32] M. Sandstedt, J. Marsh, K. Rajendran, H. Gong, S. Tao, A. Persson, et al., Improved coronary calcification quantification using photon-counting-detector CT: an ex vivo study in cadaveric specimens, Eur. Radiol. 31 (2021) 6621–6630, https://doi.org/10.1007/s00330-021-07780-6.
[33] N.R. van der Werf, S. Si-Mohamed, P.A. Rodesch, R.W. van Hamersvelt, M.J. W. Greuter, S. Boccalini, et al., Coronary calcium scoring potential of large field-of-view spectral photon-counting CT: a phantom study, Eur. Radiol. 32 (2022) 152–162, https://doi.org/10.1007/s00330-021-08152-w.
[34] L.R. McBride, K.S. Naunheim, A.C. Fiore, H.H. Harris, V.L. Willman, G.C. Kaiser, et al., Aortic valve decalcification, J. Thorac. Cardiovasc. Surg. 100 (1990) 36–43, https://doi.org/10.1016/s0022-5223(19)35596-5.
[35] M. Oliveira, L. Guittet, M. Hamon, M. Hamon, Comparative value of cardiac CT and transesophageal echocardiography in infective endocarditis: a systematic review and meta-analysis, Radiol. Cardiothorac. Imag. 2 (2020), https://doi.org/10.1148/ryct.2020190189.
[36] V. Mergen, T. Sartoretti, M. Baer-Beck, B. Schmidt, M. Petersilka, J.E. Wildberger, et al., Ultra-high-resolution coronary CT angiography with photon-counting detector CT: feasibility and image characterization, Invest. Radiol. 57 (2022) 780–788, https://doi.org/10.1097/RLI.0000000000000897.
[37] Boccalini S, Si-Mohamed SA, Lacombe H, Diaw A, Varasteh M, Rodesch P-A, et al. First In-Human Results of Computed Tomography Angiography for Coronary Stent Assessment With a Spectral Photon Counting Computed Tomography. Invest Radiol 2021;Publish Ah:1–10. 10.1097/rli.0000000000000835.
[38] M. Vecsey-Nagy, G. Tremamunno, U.J. Schoepf, C. Gnasso, E. Zsarnóczay, N. Fink, et al., Intraindividual comparison of ultrahigh-spatial-resolution photon-counting detector CT and energy-integrating detector CT for coronary stenosis measurement, Circ. Cardiovasc. Imaging 17 (2024) e017112, https://doi.org/10.1161/CIRCIMAGING.124.017112.
[39] M.T. Hagar, T. Kluemper, M. Hein, M.C. von Zur, S. Faby, F. Capilli, et al., Photon-counting CT-angiography in pre-TAVR aortic annulus assessment: effects of retrospective vs. prospective ECG-synchronization on prosthesis valve selection, Int. J. Cardiovasc. Imaging 40 (2024) 811–820, https://doi.org/10.1007/s10554-024-03050-w.
[40] N. Hirai, J. Horiguchi, C. Fujioka, M. Kiguchi, H. Yamamoto, N. Matsuura, et al., Prospective versus retrospective ECG-gated 64-detector coronary CT angiography: assessment of image quality, stenosis, and radiation dose, Radiology 248 (2008) 424–430, https://doi.org/10.1148/radiol.2482071804.
[41] Z. Sun, K.H. Ng, Prospective versus retrospective ECG-gated multislice CT coronary angiography: a systematic review of radiation dose and diagnostic accuracy, Eur. J. Radiol. 81 (2012) 94–95, https://doi.org/10.1016/j.ejrad.2011.01.070.